Optodic Bonding of Optoelectronic Components in Transparent Polymer Substrates-Based Flexible Circuit Systems

Yixiao Wang[a], Meriem Akin[b], Lisa Jogschies[b], Ludger Overmeyer[a], Lutz Rissing[b]

[a]Institute of Transport and Automation Technology, Leibniz Universität Hannover, an der Universität 2, Garbsen, Germany;
[b]Institute of Micro Production Technology, Leibniz Universität Hannover, an der Universität 2, Garbsen, Germany

ABSTRACT

In the field of modern information technology, optoelectronics are being widely used, and play an increasingly important role. Meanwhile, the demand for more flexible circuit carriers is rapidly growing, since flexibility facilitates the realization of diverse functions and applications. As a potential candidate, transparent polymer substrates with a thickness of about a hundred micrometers by virtue of their low cost and sufficient flexibility are getting more attention. Thus, accomplishing an integration of optoelectronic components into polymer based flexible circuit systems increasingly is becoming an attractive research topic, which is of great significance for future information transmission and processing. We are committed to developing a new microchip bonding process to realize it. Taking into account the fact that most economical transparent polymer substrates can only be processed with restricted thermal loading, we designed a so-called optode instead of a widely adopted thermode. We employ UV-curing adhesives as bonding materials; accordingly, the optode is equipped with a UV irradiation source. An investigation of commercial optoelectronic components is conducted, in which their dimensions and structures are studied. While selecting appropriate transparent polymer substrates, we take their characteristics such as UV transmission degree, glass transition temperature, etc. as key criterions, and choose polyethylene terephthalate (PET) and polymethyl methacrylate (PMMA) as carrier materials. Besides bonding achieved through the use of adhesives cured by the optode, underfill is accordingly employed to enhance the reliability of the integration. We deposit electrical interconnects onto the polymeric substrate to be able to bring the optoelectronic components into electrical operation. In order to enlarge the optical coupling zone from component to substrate within the proximity of the adhesive or underfill, we employ transparent interconnects made of indium-tin-oxide. We present the results of the performance tests, including the contact resistances, mechanical tests and environmental tests.

Keywords: bonding, optode, UV-curing adhesives, optoelectronic components, integration, transparent polymer substrate, flexible circuits, interconnections

1. INTRODUCTION

Since the last century, the electronics industry has developed rapidly, while light remains the key word for the future. As a technical bridge, optoelectronics with a great variety of applications in different areas is getting more and more attention [1]. Novel technologies for realizing the integration of optoelectronic components, such as Laser Diodes (LD) or Light Emitting Diodes (LED) as light sources as well as Photo Diodes (PD) as light detectors, into highly integrated circuit systems are being developed [2] [3]. In addition, people are no longer satisfied with purely conventional rigid printed circuit boards (PCB), but investigate to develop flexible integrated circuits [4]. This helps to reduce, e.g the overall thickness and weight of multilayer integrated circuits. Assembly and board-to-board connection become therefore easier and more reliable, consequently enhancing the integration level of the circuit systems. The biggest advantage benefiting from the flexible substrates is

Further author information: (Send correspondence to Yixiao Wang)
Yixiao Wang: E-mail: yixiao.wang@ita.uni-hannover.de, Telephone: 0049-511-762-18329

Smart Photonic and Optoelectronic Integrated Circuits XVII, edited by Louay A. Eldada, El-Hang Lee, Sailing He,
Proc. of SPIE Vol. 9366, 936609 · © 2015 SPIE · CCC code: 0277-786X/15/$18 · doi: 10.1117/12.2077072

the feasibility of diverse applications on flat and curved surfaces [5]. Furthermore, in terms of manufacturing, flexibility of carrier substrates allows a reel-to-reel (R2R) mass production enabling a highly-efficient fabrication process. Another requirement that the circuit carrier substrates should meet is transparency. This optical property facilitates advanced applications, such as various transparent optical sensors [6] [7]. With this in mind, transparent polymer films with a thickness up to 200 microns are particularly adapted since they have a high light transmission and provide sufficient flexibility. Moreover, most of them are low-cost, e.g. PET, PVC and PMMA. Due to their economical price the overall cost of production can thereby be reduced.

In addition to appropriate materials, we also need integration technology in order to realize flexible optoelectronic integrated circuits. Flip chip bonding technology is the state of the art for mounting and contacting electronic chips, which is widely used thanks to its efficient processing and high compactness. Subordinate to flip chip bonding, there are three main technologies: thermo-compression bonding, soldering and adhesive bonding [8] [9] [10]. However, because of the thermal property of polymers and their glass transition temperature Tg being usually below or around 100 °C, thermal loading can barely be applied on them. To solve this, we developed a novel bonding process named optodic bonding as a technology to accomplish the integration of optoelectronic components onto transparent polymer films without any thermal damages to the substrates.

Realizing circuitry on low Tg polymer films is another relevant issue for completing the integration of optoelectronic components. As interconnects, copper and silver are commonly used. In order to improve the optical transmission property even in the area of interconnections building a large optical coupling zone for light sources or detectors for sending or receiving optical signals, transparent conductive materials are attracting more research attention [11] [12]. We investigated the properties of indium-tin-oxide and deposited it on polymer films to examine its feasibility for employing it as an interconnect and subsequently test its performance.

2. MATERIALS

Flexible optoelectronic integrated circuitry consists of optoelectronic components, flexible substrates as well as conductive interconnects that are deposited on the carrier substrates. To integrate the components by using optodic bonding, UV-curing adhesives are used as bonding materials. In this section we investigate materials and characterize them for their use in the corresponding processes.

2.1 Optoelectronic components

Optoelectronic components are those electronic devices that produce, detect and control light [13]. In this work, we concentrate on the components which can be employed as light sources and detectors. Focusing on the commercially prevalent semiconductor-based Laser Diode (LD), Light Emitting Diode (LED) and Photo Diode (PD) we conducted a study with respect to their dimensions and structures for bonding. It should be noted that we are aiming at unpackaged chips of components, i.e. bare dies. The main advantage of employing bare dies is minimizing the structure of integrated systems due to their original small size in comparison to the packaged devices. In this way, flexibility can be guaranteed after increasing the integration density. Furthermore, it facilitates the alignment with those micro optical elements, such as optical waveguides as transmission structures or micro mirrors as coupling structures, which are required for various applications that our fabricated flexible integrated systems might be used for. On the other hand, however, the very small size of bare dies puts forward higher requirements for the integration technology, which poses new challenge to handling, assembling and also linking. In particular, positioning during assembly is extremely critical for guiding light into the next transmission structure. A small tilt can cause a great light loss and thus prohibit the signal transmission.

We employed the commercially available bare laser diode CHIP-650-P5 with a lasing wavelength of 655 nm. It has a dimension of $300 * 250 * 100\,\mu$m shown in Figure 1. According to the manufacturer's specification, this LD is fabricated by using the multi-step Metel Organic Chemical Vapor Deposition (MOCVD) growth process and has a structure of a strained Multiple Quantum Well (MQW). The waveguide is embedded in the middle of the top face. From the topography-layer and the 3D image in Figure 1, it can be seen, that the waveguide channel has a width of approximately 50 μm and is settled circa 1 μm lower from the upper surface. On either side of the waveguide, there is the contact pad anode. Because of the fabrication technology of the laser diode [14], the cathode lies on the opposite bottom face. Both electrodes are made of gold. The manufacturer also provides LDs with similar dimension and structure for different wavelengths, e.g, 980 nm and 1310 nm. From the structure

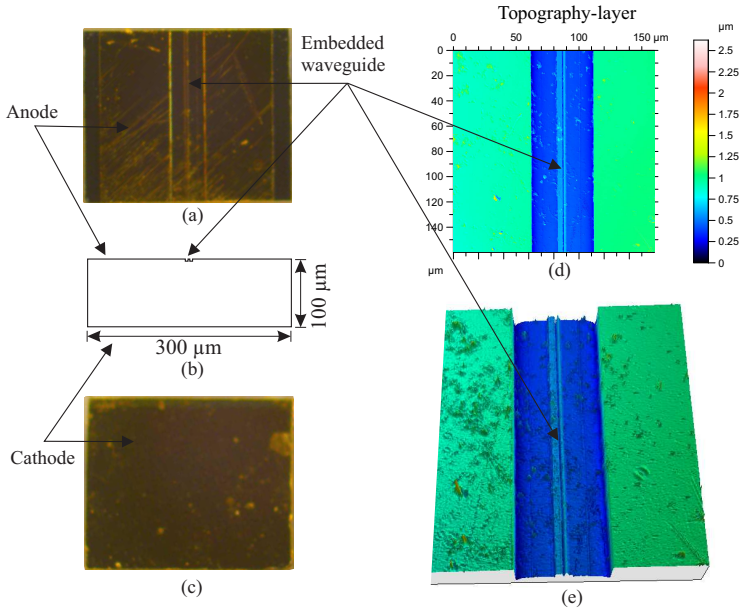

Figure 1: (a) Anode, (b) side-view, (c) cathode, (d) topography-Layer of upper face and (e) 3D image of commercially available laser diode CHIP-650-P5

of the embedded channel for the waveguide, it can be recognized that this LD emits light from its edge, which allows a simple butt coupling for further light transmission. However, due to the extreme narrow waveguide and a few microns embedded in the LD, positioning and light coupling is still a big challenge. In driving this LD a typical emitting power of 5 mW can be reached when being electrically operated with 29 mA and 2.2 V. Contrary to the edge-emitting LD, the vertical-cavity surface-emitting laser (VCSEL) is another type of semi-conducted LDs, which emits a laser beam perpendicular from the top surface [15]. Both electrodes of VCSEL are mostly located on the same face, which allows interconnection realized by applying flip chip bonding technology.

In addition to investigating and identifying LDs, we also studied the dimension and the structure of LEDs and PDs. As above mentioned, in order to realize a transmission path by only using butt coupling, an edge-emitting LD is preferred. Analogously, employing an edge illumination photo diode simplifies and facilitates light coupling without utilizing optical components for changing the light direction. PD KPEIMC-UDCOM has a dimension of $450 * 450 * 250$ μm and with its wide photodetecting area of about $100 * 120$ μm on the edge it can be illuminated by butt coupling. For testing applications by establishing a complete optical transmission path, LDs or LEDs as light sources should provide a wavelength range for emission as close as that for detection of a photo diode. For example, LD CHIP-1310-P5 with a wavelength of 1310 nm matches PD KPEIMC-UDCOM with a high responsivity at the wavelength of 1310 nm.

2.2 Test Chip

Electric conductivity is an important criterion to evaluate the quality of bonding. However, it cannot be easily measured at the bonding junction of the diode. Thus, we employed a test chip, which allows a direct resistance measurement. The chip has a larger size of $950 * 950$ μm than that of bare LD dies and a similar thickness of 150 μm. Figure 2 (a) shows its layout. There are 20 contact pads made of aluminum with a dimension of $80 * 80$ μm on the chip. 5 μm electroless Nickel-Gold bumps are provided on the pads. According to the layout of the chip, we designed the test circuit (Figure 2 (b)). A stencil mask (Figure 2 (c)) with 25 patterns of test circuits was fabricated for coating interconnects on the polymer film using the process introduced in Section 5. The test chip is designed with two pairs of Kelvin sensing structures on the main diagonal, which enables a precise measurement of the contact resistance by using the four-point probe method. As seen in Figure 2 (b), the bonding junctions of two pads, marked with white circles in the Kelvin sensing structures, are to be measured.

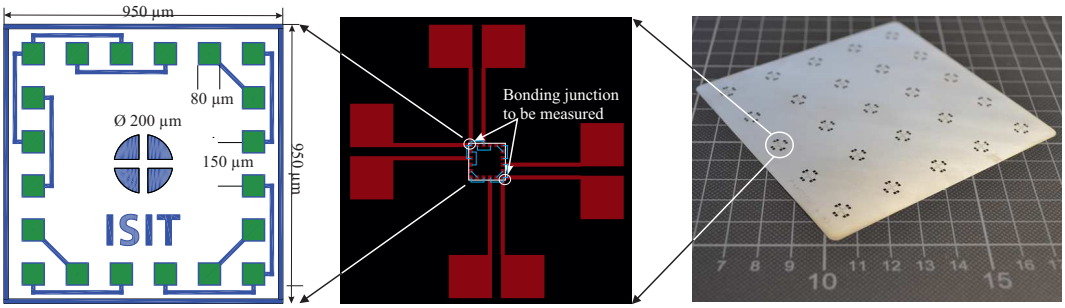

Figure 2: (a) Layout of test chip; (b) correspondingly designed test circuit on polymer film and (c) stencil mask

2.3 Transparent polymer films

As introduced, regarding the sufficient flexibility and economical price, we employed polymer films as circuitry carrier substrates. The thickness of the films is limited to 200 μm in this work. When selecting the first testing materials, we mainly took properties of the UV transmission degree and the glass transition temperature (Tg) into account.

Through an investigation of the UV transmission degree of the polymer substrates, the transmission window for UV irradiation can be estimated. This helps us to choose an appropriate UV irradiation source for the optode. Measurements exhibit that PET has a nearly constant transmission degree of about 85 % in the range from 350 nm to 400 nm, while PMMA shows an increase of the transmission degree along with the increasing wavelength. At the wavelength of about 387 nm, both films reach a transmission degree of almost 90 %.

The glassliquid transition (or glass transition in short) is the reversible transition of amorphous materials (or in amorphous regions within semicrystalline materials) from a hard and relatively brittle state into a molten or rubber-like state [16]. Knowing the temperature at which this transition occurs, helps to define the thermal budget that is allowed to be loaded during processing. The polymer films begin to deform when being processed with a temperature close to or above Tg for a certain duration. Investigation shows that PET has a Tg of 70 °C, while PMMA has a little higher Tg of 105 °C. Overall, both indicate a strongly restricted thermal loading.

2.4 Transparent electrical interconnects

In order to enable an efficient optoelectronic integrated system, we strive to minimize sporadic scattering of light through the electrical interconnects in proximity of the active emissive and detective regions of the optoelectronic components. In order to structure the interconnects, we employ a transparent electrically conductive oxide – indium tin oxide (In_2O_3:Sn), which we refer to henceforth as ITO. In particular, thin films (< 1 μm) of ITO are able to exhibit simultaneous low electrical resistivity and high optical transparency when utilizing the proper coating technique e.g. as investigated by S. Ishibashi et al. [17] [18]. In this work, we employ RF magnetron sputter deposition to coat the polymeric substrates described in Section 2.3. Based on sputtering experiments of ITO on borosilicate glass, the work of Azevedo et al. [19] on PMMA and the work of M. Boehme et al. [20] on PET, we identified suitable sputtering conditions for our application as given in Table 1. Most notably, tempering of deposited ITO coatings for enhancing electrical and optical quality is not possible due to the thermo-mechanical restriction imposed by the glass transition of the polymeric substrates.

We characterize a continuous deck of ITO of a 1 μm thickness as deposited on borosilicate glass for quasi substrate-independent properties. Employing a four-point probe, specific electrical resistivity was measured to be in the range of 2-4 mΩcm. Besides, the opacity of the ITO layer at a wavelength range of 200-1200 nm was obtained by means of UV-Vis-NIR spectrophotometry (Figure 3). In particular, the best transmittance of 74.7 % is obtained at 770 nm. In terms of substrate-dependent properties such as the structure of deposition growth, surface roughness and adhesion between coating and substrate, we characterize a continuous deck of ITO of a 1 μm thickness as deposited on PMMA and PET. First, a scotch tape test on ITO layers deposited onto PMMA and PET substrates confirms indefectible adhesion between ITO and polymeric substrate. Due to the low thickness of ITO and non-resistance of PMMA and PET to abrading, the scratch adhesion test fails.

Table 1: Conditions of sputter deposition

Condition	Value
Target size (in)	6.5
Target to substrate distance (mm)	70
Sputter power (W)	40
Gas	Ar
Air flow (sccm)	50
Start pressure (mbar)	e^{-6}
Sputtering pressure (mbar)	e^{-3}
Deposition temperature (°C)	20
Deposition rate ($\frac{nm}{min}$)	3

Next, the micro-topology of the ITO coating is inspected by means of atomic force microscopy (AFM). As

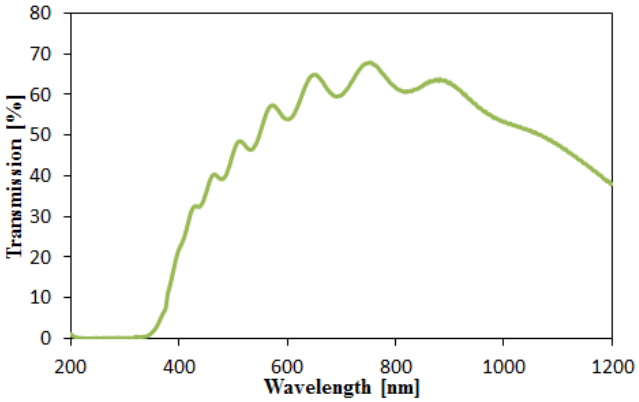

Figure 3: Optical transmission of a 1 μm thick ITO layer deposited on borosilicate glass at conditions listed in Table 1

shown in Figure 4, the sputtered ITO layers exhibit the Volmer-Weber growth mechanism [21] and Movchan-and-Demchishin topological model [22] ($\frac{\text{Temperature of substrate during sputtering}}{\text{Melting temperature of ITO}} < 0.26$) on all substrate materials. However, the nucleated three-dimensional islands are of a smaller area size when deposited on PET

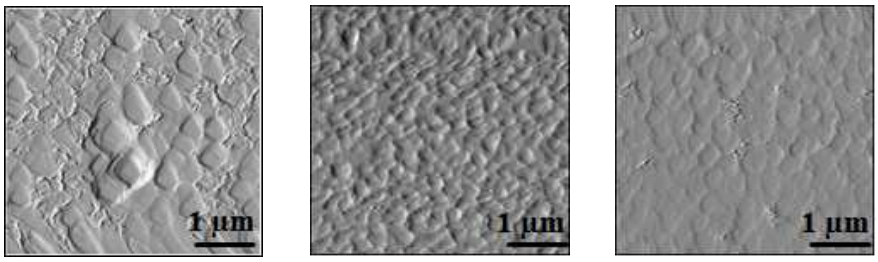

(a) (b) (c)

Figure 4: (a) Atomic force micro-graphs of a 1 μm thick ITO layer deposited on glass, (b) PET and (c) PMMA.

whereas nucleation is of an equal area distribution on PMMA and borosilicate glass. Besides, it falsely appears that deposition on polymeric substrates delivers flatter ITO coatings. The latter artifact is attributed to a non-uniform deposition across the entire substrate area as the AFM measurements were not conducted at the exact same locations for all substrates.

2.5 UV-curing adhesives

In order to integrate the optoelectronic components into polymer films with the lowest possible thermal loading, we decided to employ UV-curing adhesives as bonding materials. Generally, there are three different types of electrically conductive adhesives, which are used in the industry of circuits fabrication: isotropic conductive adhesive (ICA), anisotropic conductive adhesive (ACA) and non-conductive adhesive (NCA) [23]. Most adhesives consist of a base, which is made from polymer, such as epoxy, acrylate, and fillers from a variety of materials depending on the applications [24]. Adhesives of all these three types used in the industry are mostly hardened by loading thermal energy. In contrast, UV-curing adhesives containing photo-initiators are hardened by an exposure to UV radiation. It is because of this curing principle that UV-curing ICAs and ACAs are barely found on the commercial adhesive market, since the radiation directed to the adhesives can be strongly reflected due to fillers. Usually, UV-curing adhesives can be hardened more quickly than those, which are thermally cured.

So far, a dual UV- and thermal curing ICA has been developed on the market, which is later referred to as adhesive F. It is filled with silver particles. Curing with UV-radiation in the wavelength range of 320 - 400 nm enables a quick fixation for 1-5 seconds and afterwards, it must be cured with heat for a permanent and maximum adhesion. Nevertheless, it requires a thermal loading at a low temperature, which can be regulated down to 80 °C by employing a longer curing time of 30 min. However, using ICAs for bonding ICs with a high contacts density, a short circuit can easily be caused. Moreover, after the curing of the ICA, underfill is necessary to fill the space between the chip and the substrate, so that the mechanical fixation can be guaranteed. Compared to ICAs, UV-curing NCAs are commercially easily acquired and in this work, a NCA refereed to as adhesive A is employed. Dispensing NCAs has fewer requirements since no short circuit can be caused. Thus, the NCA can be applied on the entire surface of the contact spot and at the same time serve as underfill, hence saving the step for dispensing underfill. In addition, employing NCAs provides a possibility of choices for the desired transparency enabling a high transmission of light to adopt various applications. However, while employing NCAs, the chips or ICs are commonly required to be bumped in order to establish the electrical connection.

3. OPTODIC BONDING

The integration technology "optodic bonding" is based on conventional flip chip die bonding. The name derives from the optode, which is analogous to the commonly used thermode and functionally serves as a light source. The first concept of optode was introduced in [25]. Further developments and improvements relating to the functionality to be implemented and the convenience of usage are forwarded in this work.

3.1 Optode Setup

The concept of the optode shown in Figure 5 is compatible for both variations: The sideway optode and the optode for irradiation from the bottom. On the basis of the sideway optode, whose setup and working principle has been introduced in detail in [26], the optode for irradiation from the bottom is realized and integrated in the same setup. By equipping two LED-UV lamps on the side and employing a mirror with an average UV reflectivity higher than 96 %, the setup is used as a sideway optode, while it is used as an optode for irradiation from the bottom when employing a transparent glass with a high UV transmission degree instead of the UV-reflective mirror and placing a LED-UV lamp under the glass. With respect to the optode from the bottom, UV irradiation is emitted from the LED lamp, passes through the transparent glass and subsequently through the polymer film, and finally reaches the contact spot, where the UV-curing adhesive lies. According to the investigation of UV irradiation technology [26] we employed the same UV-LED lamp with a wavelength of 385 nm adopted to the UV transmission property of PMMA and PET (Section 2.3) as the irradiation source for the optode from the bottom as for the sideway one. To change the irradiation direction by 90°, we installed a so-called side lens on the head of the LED lamp. In addition to this, the side lens has also the effect to focus the UV irradiation. The working distance between lens and contact spot should be adopted in accordance with the specification provided by the manufacturer.

The optode should be integrated into a manual flip chip die bonding assembly system. The integration can be realized by designing an underplate to replace the heat plate which serves as a thermode. As introduced

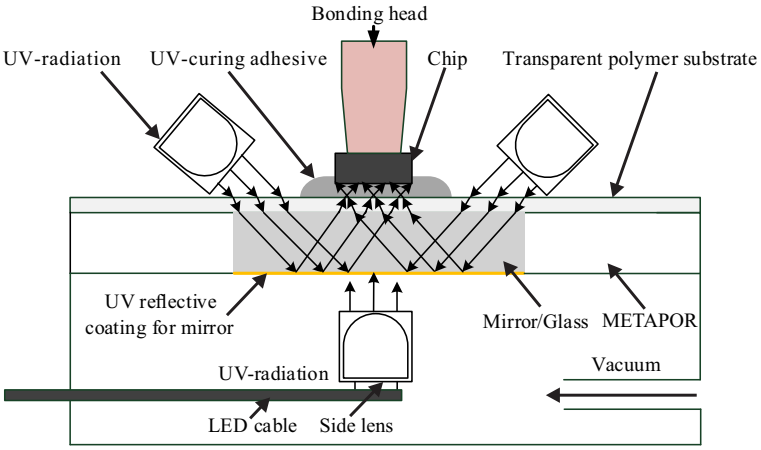

Figure 5: Schematic illustration of optode

in [26], this underplate has to provide the vacuum function to get the lightweight and flexible polymer films fixed onto the surface. It helps to maintain the positioning accuracy of small components during the bonding process. In [26], the vacuum was realized by building a channel in shape of a circle consisting of small holes around the contact spot on the surface of the underplate, which, however, resulted in an inhomogeneous vacuum function. It can be seen that the polymer film bows in the middle or tilts at the edge. Improvement can be made by employing the METAPOR, which is made of porous aluminum composite material especially for vacuum and compressed air.

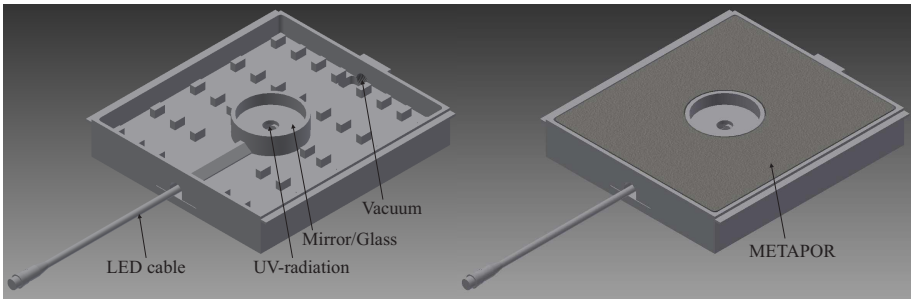

Figure 6: Design of underplate

The realized underplate and a photo taken during the optodic bonding process using the optode for irradiation from the bottom are respectively shown in Figure 7 (a) and Figure 7 (b). For the sideway optode, an x-y-z stage for carrying the UV source and adjusting its position as well as a gadget for adjusting the incidence angle of UV radiation were designed and realized [26]. This extra unit takes up a certain operation space in the assembly system and increases the default pressure applied on the bonding head, which therefore has to be calibrated beforehand. However, it is precisely because of this extra unit for adjustment of UV radiation, that the difficulty of alignment among the three objects, the UV source, the circuits on polymer films and the dies to be bonded, can be greatly reduced. An optimum position between the UV lamp and the bonding head has previously been found out by adjusting the extra unit before bonding, which means, the alignment between the UV source and the dies has been completed. Since the UV source is not fixed on the underplate, it can be considered as flexible and subsequently aligned according to the position of the circuit on polymer films as long as the circuit is still located within the boundary of the mirror. In this way, the alignment of these three objects is separated into two independent steps, which is much easier to handle than one combined step. In the contrast, no extra unit is necessary for fixing or adjusting the UV source in the optode for irradiation from the bottom, because the UV source is fixed under the middle of the glass. Consequently, the alignment of UV source, substrate and

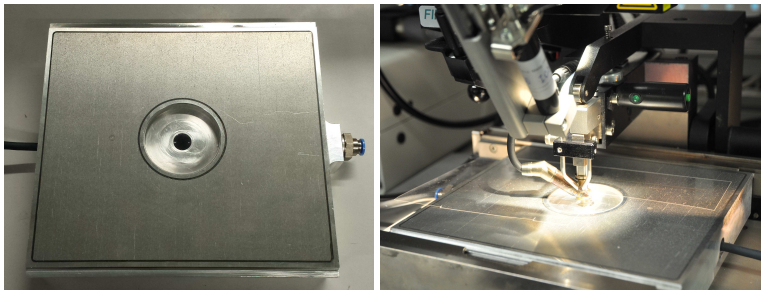

(a) (b)

Figure 7: (a) realized underplate; (b) photo of optodic bonding using optode for irradiation from the bottom

dies has to be done in one step. Nevertheless, the alignment difficulty can be compensated by employing a side lens with a bigger diameter, which enlarges the effective area of alignment. The distance between side lens and adhesive on the underplate is 13 mm. Manufacturer's specification says that for this working distance, a side lens with a diameter of 6 mm provides an intensity of about 3200 mW/cm^2 in a circle with a diameter of appr. 3 mm disregarding any losses which might be induced later due to added components in between. This effective area with a diameter of 3 mm can be enlarged by employing a side lens with a diameter of 10 mm providing an average intensity of appr. 800 mW/cm^2 in a diameter of 6 mm. Although the maximum intensity of UV radiation is reduced as the diameter of the side lens increases for a certain working distance, the minimum required irradiation energy can always be met by choosing appropriate combinations of process parameters: the irradiation intensity and duration. Take the adhesive A as an example: according to the data sheet, 10 seconds irradiation time is required for a full cure if using a lamp with an intensity of 200 mW/cm^2. The intensity provided by a side lens with either 6 mm or 10 mm meets this requirement. Analogously, to save process time, the irradiation duration can be shortened accordingly by increasing the irradiation intensity.

3.2 Procedures of optodic bonding

Optodic bonding contains five main procedures. First of all, materials are to be prepared as commonly done. Bonding is implemented in a laboratory with a constant temperature of 21.7 °C. The UV-curing adhesives, which are stored in a cool place, e.g. the adhesive A, must be conditioned to this room temperature before use. Another important preparation is the cleaning and drying of the surface of polymer films to be bonded. To begin the bonding, the chip is faced down aligned with the bonding head. With the help of vacuum in the bonding head the chip is picked up and stuck on the head by 180° with the active side upwards. The polymer circuit carrier is placed on the underplate and correspondingly aligned with the contact pads on the active side of chip. Next, the UV-curing adhesive is to be dispensed on the traces of the polymer film. As seen in Figure 7 (b), the adhesive cartridge is fixed in a front-dispenser, which can be pushed down closely onto the polymeric substrate. For a convenient replacement of used adhesives, we applied the time-pressure dispensing process. In order to improve the accuracy and the reproducibility of the dispensed volume, an advanced dispensing device was adopted, which utilizes a continuous measurement and a real-time evaluation of the air pressure as well as a constant monitoring of the fluid temperature to achieve a precise dispensing. During and after the application of the adhesives, it should be noted that the polymeric substrate remains unmoved with the help of vacuum on the underplate and that the traces of circuit on the substrate are still correctly aligned with the contact pads on the chip. Only after this confirmation, the bonding head can be pivoted down slowly onto the contact spot of the polymer film. Bonding will be completed in the last step by curing UV adhesives with the additional assistance of applied pressure on the bonding head. The process parameters, such as UV irradiation intensity, irradiation time and applied pressure, have significant effects on the bonding results.

4. BONDING OF THE BARE LASER DIODE

In Section 2.1, the bare laser diode CHIP-650-P5 was introduced. As mentioned, employing this edge-emitting LD, a fully operational light transmission structure can preliminarily be established by adopting butt coupling,

which has the advantage of avoiding the use of extra coupling elements. We employed this LD as a light source and realized its integration in the polymer-based circuit system by applying the above presented optodic bonding. However, as depicted in Figure 1, the LD has its contact electrodes on two opposite faces, which means, the electrical integration cannot be completed in one step by only using optodic bonding. To solve this, we additionally adopted the micro dispensing process to contact its second electrode. The whole bonding procedure is illustrated in Figure 8.

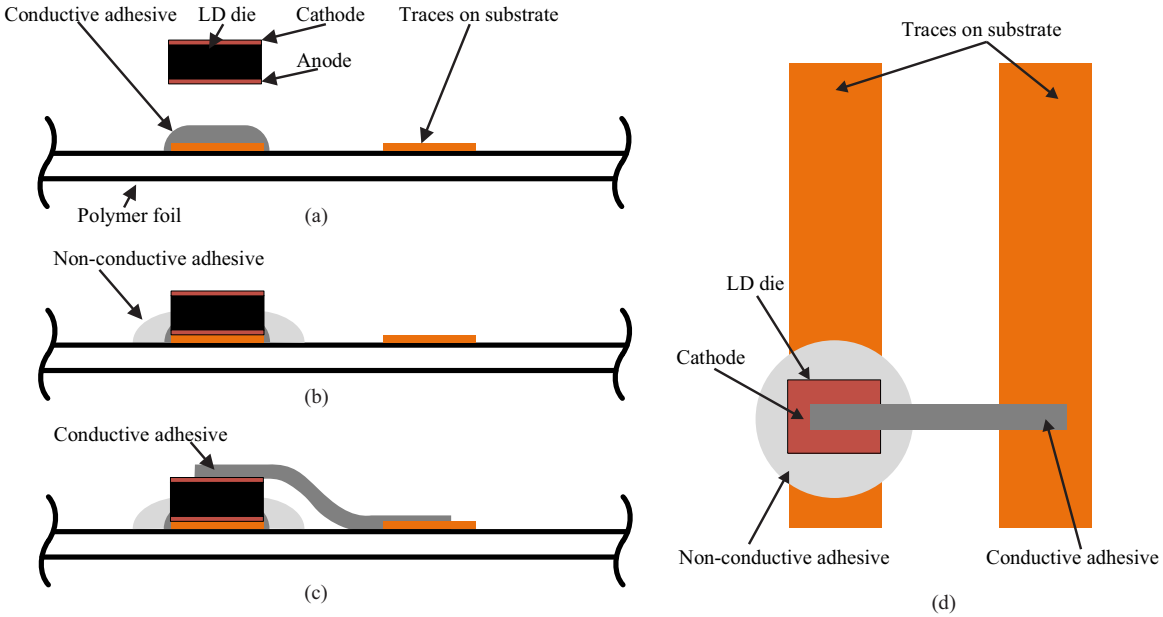

Figure 8: (a) Mounting and contacting of anode using optodic bonding; (b) Applying of non-conductive adhesive as underfill and insulating layer; (c) Contacting of cathode using micro dispensing; (d) Top view of the bonded LD

In step (a), we carried out the process of optodic bonding described in Section 3.2 to mount the LD die on the polymer-based substrate and meanwhile realize a connection between the first electrode (anode) and the conductive traces of the circuit. As bonding material, we hereby employed the previously introduced adhesive F, which is isotropic conductive and should be cured firstly with UV irradiation and finally with a thermal treatment at a low temperature for a maximum adhesion. The main reason for employing ICAs lies in the thin metalization pad made of gold on the electrode without any bumps. In this case, employing NCAs would not ensure the electrical connection between the LD and the circuit. Moreover, this LD die is all-over metalized on both faces, which simplifies the dispensing process. No more attention should be paid, since there is only one pad on each face and no danger of short circuit can be induced because of imprecise dispensing or spreading of adhesive A. As the next step, NCA A was applied to completely cover the ICA F around the bonded die, and especially the gap between the two traces. Although no short circuit can be caused on the same surface, it can still occur, that the anode contacts with the trace, with which the cathode is supposed to be contacted through the dispensing in step (c). Therefore, the NCA hereby serves as an insulating layer. In addition, the NCA is utilized as underfill to enhance the mechanical strength of the mounting which is commonly desired for an ICA bonding. In the last step, the cathode is to be electrically contacted with the polymer-based circuit. This is realized by employing ICA F again, which should be slowly and continuously dispensed from the upper face of the LD onto the trace on the right hand side (Figure 8 (d)). Since fabrication of integrated circuits tends to be smaller and denser, the space between the conductive traces is expected to stay narrow for a higher integration level. With this in mind, a short circuit can be easily caused during step (c) when leaving out step (b).

In order to successfully drive the LD, process parameters should be properly set according to the materials. In step (a), where optodic bonding was used, we decided for an optode from the bottom rather than a sideway

optode with an extra unit since the LD is small and fragile and cannot bear a big bonding force. The optode from the bottom reduces the danger of the chip being crushed. The bonding force is correspondingly adjusted to 5 N. The diameter of the side lens used for the optode from the bottom was 6 μm, which is big enough for a flexible positioning of the LD. For curing ICA F, we set the UV irradiation intensity to 50 % (corresponds to appr. 1600 mW/cm^2) and the irradiation time to 5 seconds. In step (b) for employing NCA A, the irradiation intensity was set to 90 % (appr. 2880 mW/cm^2) and the irradiation time to 10 seconds, so that a complete curing effect can be guaranteed. In step (c), a low-temperature thermal treatment of 80° was carried out in an oven lasting 30 minutes for a final adhesion of the used ICA. Figure 9 shows a microscopy image, where the anode of the LD is bonded upwards. In its applications, this should be decided according to the dimension of the employed transmission structures, with which the LD is to be coupled. For electrically driving the LD, we

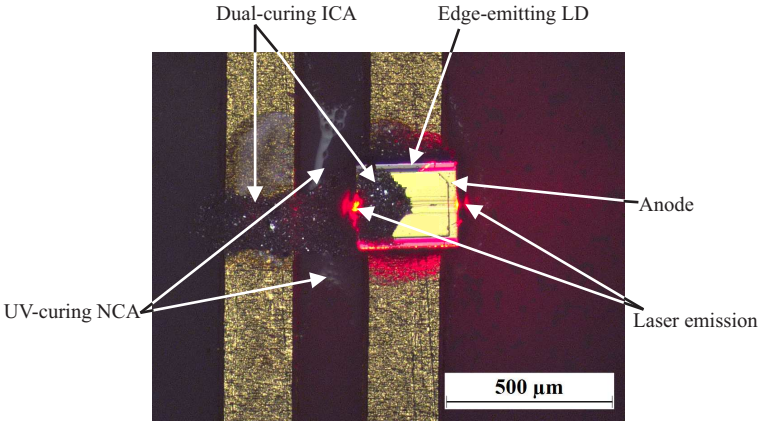

Figure 9: Active edge-emitting laser diode

used the power supply device, which provides a stable voltage. By applying 2.2 V, the device indicates a current floating around 7 mA which is far lower than the expected value of 29 mA given on the data sheet. It might be due to the lack of a driving circuit for attaining a constant current with a temperature regulation or alternatively a power control.

5. STRUCTURING OF ELECTRICAL INTERCONNECTS

In this work, we avoid any chemical degradation of the polymeric substrate that may be induced through photo-lithography processes. Alternatively, we employ a shadow masking technique to deposit structured ITO interconnects on PET and PMMA. Here, the layout of electrical interconnects is repeatedly laser-cut into 100 μm-thick steel sheets (Figure 2 (b) and (c)), which we employ as a freestanding stencil mask during the sputter deposition. In order to obtain well-defined and short-free interconnects, we cope with the mechanical flexibility of the polymer film when freestanding. Thus, we investigated various clamping approaches to enforce a unitary assembly between stencil mask and polymer film. First, we employed clamping plates of various thicknesses (Figure 10 (a)) with compact cavities in the clamp emplaced around the structures of the shadow mask. On the one hand, the pattern spreading is alleviated [27], and the deposited structures obtain more distinguishable boundaries, yet not short-free, with increasing thickness of the clamping plate (a selection of the sputtering results is depicted in Figure 10 (c) and 10 (d)). On the other hand, the deposition rate decreases with increasing thickness of the clamping plate affecting the throughput efficiency of the coating process excessively.

Consequently, we substituted clamping by mass through magnetic clamping [28] (Figure 11 (a)) to obtain a superior sharpness in edge definition while not deteriorating the deposition throughput. Here, we employed a ferrite magnet of Y30-grade (B_r=380-400 mT) that is stable at temperatures up to 250°C. Due to the thickness of the ferrite magnet, the target-to-substrate distance decreases by 20 mm. Therefore, the deposition rate is expected to be higher than 3 $\frac{\text{nm}}{\text{min}}$, which is beneficial in terms of process efficiency. Besides, the substrate cooling mechanism during sputtering, which is integrated in the anode plate, is not efficiently transferred through

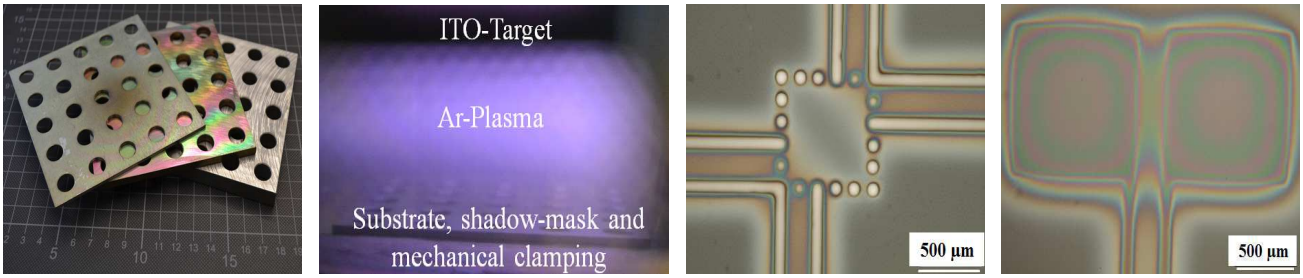

(a) (b) (c) (d)

Figure 10: (a) Mechanical clamping plates of various thicknesses 2 mm, 5 mm and 10 mm, (b) sputter deposition on mechanically-clamped mask and polymer film and (c) detailed micro-graphs of the resulting structured ITO coating.

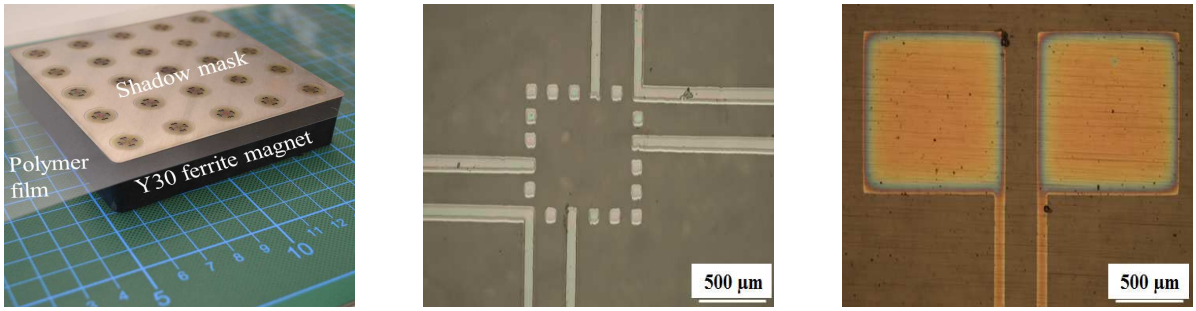

(a) (b) (c)

Figure 11: (a) Clamping setup by means of the ferrite magnet, (b) (c) detailed micro-graphs of the resulting structured ITO interconnects

the magnet onto the polymer film. Therefore, continuous and extended sputtering, despite a low sputtering power, subjects the polymer film to overheating and the ITO layer to cracking due to mismatches of coefficients of thermal expansion (Figure 12). That is why, enforcing polymer relaxation during sputtering is necessary

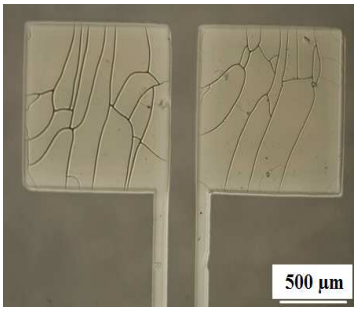

Figure 12: Cracks in ITO pads due to overheating of the polymer film and mismatches of the coefficients of thermal expansion.

for obtaining crack-free ITO films. In particular, during sputtering, we employ a rotating anode plate at a rotational speed of 1 rotation per minute. Here, the substrate is effectively exposed to sputtering for 5 seconds per rotation. Hence, relaxation of the polymer film is allowed to happen in the remaining exposure-free 55 seconds of the rotation. Ultimately, we obtain short-free and crack-free interconnects (Figure 11 (b) and 11 (c)).

6. RELIABILITY

In order to investigate the feasibility of the structured ITO interconnects on PMMA and PET, we focused on two essential performances of the bonding junction: the electric resistance and the mechanical strength. A test chip introduced in Section 2.2 was utilized and accordingly, a test circuit (Figure 2 (b)) described in Section 5 was employed. By applying optodic bonding, the test chip was mounted and contacted with the test circuit on PMMA and PET substrate coated with ITO. Bonding tests were carried out in a laboratory with a constant temperature of 21.8 °C and a humidity of 42 %. NCA A was used. The UV irradiation intensity and irradiation time were set to 90 % and 10 seconds. A force of 5 N was applied on the bonding head. The rear side of the bonded chip can be observed clearly thanks to the transparency of the employed carrier substrates PMMA and PET. As an example the chip on PMMA is shown in Figure 13 (a).

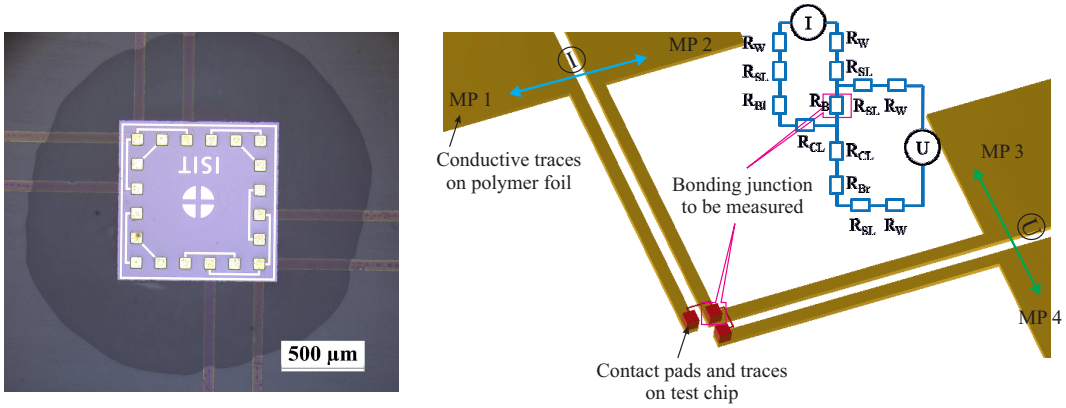

(a) (b)

Figure 13: (a) Rear side of bonded chip on ITO structured PMMA substrate; (b) electric resistance measurement using 4-point probe method. R_W: resistance of connection wires; R_{SL}: trace resistance on the substrate; R_{CL}: trace resistance on the chip; R_{Bl}, R_B, R_{Br}: resistance of the left bonding junction, middle bonding junction and right bonding junction

In order to measure the electric conductivity of the bonding junction accurately, the four-point probe method is preferred. The measurement principle is illustrated in Figure 13. Constant current is supplied between measuring point 1 (MP1) and measuring point 2 (MP2), the induced voltage can be consequently measured between MP3 and MP4. As explained in the equivalent circuit in Figure 13, the bonding junction, which is marked with magenta, is the only common part of the two current and voltage pathways. The resistance of this bonding junction can be calculated by the measured voltage divided by the supplied driving current. The advantage of using the four-point probe method over the two-point probe is that the former excludes the voltage drop across the connection wires, along the conductive traces, etc. during measuring and indicates a negligible error induced by the measurement setup [29].

Firstly, by checking the conductivity of the adjacent contact pads, e.g. MP1 and MP2 or MP3 and MP4, from a large amount of test samples using the 2-point probe, we confirmed the survival rate of the bonding junctions. The test chips bonded on PMMA showed a survival rate of 92.75 %, while a survival rate of 95 % was reached on PET. Next, we measured the electric resistance of the bonding junctions using the 4-point probe method. The best result indicated a resistance of 0.34 Ω. In addition, for investigating the mechanical strength we implemented shear tests, in which a maximal kilogram-force (kgf) of 2.15 was measured. Regarding the area of the test chip of approximately 1 mm^2, a mechanical strength of circa 21.5 N/mm^2 can be achieved. Overall, these performances exhibit a convincing reliability. However, the environmental test revealed a weak resistance against extreme environmental conditions. Given the Tg of PET the test temperature was set to 60 °C and the relative humidity was controlled at 85 %. The test lasted 24 hours. Although a lower test temperature was chosen, an obvious deformation of the PET film can be observed. In contrast, the PMMA film remained a

planar substrate. The main reason for the degradation is probably the high humidity, which should be further investigated.

7. CONCLUSION AND OUTLOOK

In this work we presented a novel bonding process, the so-called optodic bonding as an integration technology to realize the mounting and contacting of commercially available optoelectronic components into transparent polymeric substrate-based flexible circuits. A highlight of optodic bonding is the design of an optode as a light driving source in contrast to the widely used thermode and correspondingly, adopting UV-curing adhesives as bonding materials. It opens the way for employing thermally sensitive materials as carrying substrates of circuit systems, such as thin and transparent polymer films. For instance, a bare laser diode was successfully bonded by optodic bonding plus micro dispensing process using dual curing ICAs and UV-curing NCAs. Considering the benefits of using transparent interconnects for establishing an optical transmission path, the feasibility of the structured ITO interconnects on the polymeric substrates for realizing integrated circuits was investigated. A proper test chip was utilized. A test circuit was correspondingly designed and fabricated by applying RF magnetron sputter deposition on PET and PMMA. Measurements regarding the electric conductivity and mechanical strength of the junctions between the test chip and the test circuit produced by optodic bonding were carried out. The results show a good reliability of the ITO interconnects and great potential to be employed in optical applications.

A further optimization of optodic bonding is to be made. In particular, the setup of the optode from the bottom is to be improved in e.g. reducing the loss of UV irradiation and facilitating the alignment among the radiation source, circuit substrate and chips to be bonded. Besides, the pressure applied on the bonding head should be calibrated, especially for the sideway optode, which requires an extra unit on the sides. Transparent ITO interconnects, particularly in terms of improving their reliability, are to be further investigated of being employed well for enlarging the optical coupling zone and thus increasing the coupling efficiency. Future work is also planned on realizing the integration of other optoelectronic components, such as VCSELs, or PDs. Through selecting appropriate combinations of light sources and detectors, a transmission path adopting an optical waveguide is expected to be established.

ACKNOWLEDGMENTS

We gratefully acknowledge financial support from the Deutsche Forschungsgemeinschaft (DFG) within the framework of the Collaborative Research Center Transregio 123 - Planar Optronic Systems (PlanOS). The authors would also like to acknowledge Jakub Krischik for his support with the sputtering experiments of ITO onto glass substrates, and thank Manuel Fernández for his contribution in realizing the optode.

REFERENCES

[1] Kumar, D. M., "Optoelectronic devices & their applications," *Electronics for you* (2003).
[2] Gao, J., [*Optoelectronic Integrated Circuit Design and Device Modeling*], Higher Education Press, 4 Dawai Dajie, Xicheng District, Beijing, 100120, P.R. China, 1 ed. (2011).
[3] Zimmermann, H., [*Silicon Optoelectronic Integrated Circuit*], Springer (2004).
[4] Macleod, P., "A review of flexible circuit technology and its applications," *Prime Faraday Technology Watch* (June 2002).
[5] J.Fjelstad, [*Flexible Circuit Technology*], TN: BR Publishing, Inc., Knoxville, third ed. (2007).
[6] Matusevich, V., Wolf, F., Tolstik, E., and Kowarschik, R., "A transparent optical sensor for moisture detection integrated in a pq-pmma medium," *IEEE PHOTONICS TECHNOLOGY LETTERS* **25, No.10**, 969–972 (2013).
[7] Kim, Y., Park, S., Park, S. K., Yun, S., and Kyung, K.-U., "Transparent and flexible force sensor array based on optical waveguide," *Optics Express* **20, N0.13**, 14486–14493 (June 2012).
[8] Lau, J. H., [*Low Cost Flip Chip Technologies*], McGraw Hill Professional (2000).
[9] Tong, H.-M., Lai, Y.-S., and Wong, C., [*Advanced Flip Chip Packaging*], Springer (2013).
[10] Burghartz, J., [*Ultra-thin Chip Technology and Applications*], Springer (2010).

[11] Wu, Z., Chen, Z., Du, X., Logan, J. M., Sippel, J., Nikolou, M., Kamaras, K., Reynolds, J. R., Tanner, D. B., Hebard, A. F., and Rinzler, A. G., "Transparent, conductive carbon nanotube films," *Science* **305**, 1273–1276 (August 2004).

[12] Lee, J.-Y., Connor, S. T., Cui, Y., and Peumans, P., "Solution-processed metal nanowire mesh transparent electrodes," *Nano Lett* , 689–692 (January 2008).

[13] Sum, S.-S. and Dalton, L. R., [*Introduction to Organic Electronic and Optoelectronic Materials and Devices*], CRC Press Taylor & Francis Group (2008).

[14] Gupta, P. K. and Khare, R., [*Laser Physics and technology*], Springer (2014).

[15] Michalzik, R. and Ebeling, K. J., [*Operating Principles of VCSELs*], University of Ulm, Optoelectronics Department.

[16] [*ISO 11357-2 Plastics Differential scanning calorimetry (DSC) Part 2: Determination of glass transition temperature*] (1999).

[17] Ishibashi, S., Higuchi, Y., Ota, Y., and Nakamura, K., "Low resistivity indium-tin oxide transparent conductive films. i. effect of introducing h_2o gas or h_2 gas during direct current magnetron sputtering," *Journal of Vacuum Science and Technology* **8, no.3**, 1399–1402 (Jun. 1990).

[18] Ishibashi, S., Higuchi, Y., Ota, Y., and Nakamura, K., "Low resistivity indium-tin oxide transparent conductive films. ii. effect of sputtering voltage on electrical property of films," *Journal of Vacuum Science and Technology* **8, no.3**, 1403–1406 (Jun. 1990).

[19] Azevedo, S., Dieguey, L., Carvalho, P., Carneiro, J., Teixeira, V., Martinez, E., and Samitier, J., "Deposition of ito thin films onto pmma substrates for waveguide based biosending devices," *Journal of Nano Research* **17**, 75–83 (Feb. 2012).

[20] Boehme, M. and Charton, C., "Properties of ito on pet film in dependence on the coating conditions and thermal processing," *Surface and Coating Technology* **200, no.1-4**, 932–935 (Mar. 2005).

[21] Oura, K., Lifshits, V. G., Saranin, A., Zotov, A. V., and Katayama, M., [*Surface Science: An Introduction*], Springer (2003, XII).

[22] Movchan, B. A. and Demchishin, A. V., "Investigations of the structure and properties of thick ni, ti, w, al2o3 and zro2 vacuum condensates," *Fizika Metallov i Metaallovedenije (Physics of Metals and Metallography)* **28, no.4**, 653 (1969).

[23] Gomatam, R. and Mittal, K. L., [*Electrically Conductive Adhesives*], Koninklijke Brill NV (2008).

[24] Licari, J. J. and Swanson, D. W., [*Adhesives Technology for Electronic Applications: Materials, Processing, Reliability*], Elsevier Inc., 225 Wyman St, Waltham, MA 02451, USA (2011).

[25] Heiserich, G., Franke, S., Fahlbusch, T., and Overmeyer, L., "Optode based flip chip bonding on transparent flexible substrates," *Proc. 2nd CIRP Conference On Assembly Technologies and Systems, Toronto*, 469–477 (2008).

[26] Wang, Y. and Overmeyer, L., "Low temperature optodic bonding for integration of micro optoelectronic components in polymer optronic systems," *2nd International Conference on System-Integrated Intelligence: Challenges for Product and Production Engineering (SysInt), Bremen, Procedia Technology Elsevier*, 547–556 (2014).

[27] Tiggelaar, R. M., Berenschot, J. W., Elwenpoek, M. C., Gardeniers, J. G. E., Dorsman, R., and Kleijn, C. R., "Spreading of thin-film metal patterns deposited on nonplanar sufaces using a shadow mask micromachined in si (110)," *Journal of Vacuum Science and Technology* **25, no.4**, 1207–1208 (Jun. 2007).

[28] Ingle, F., "A shadow mask for sputtered films," *Review of Scientific Instruments* **45, no.11**, 1460–1461 (Nov. 1974).

[29] Fretz, M. and Durante, G. S., "Simulation of daisy chain flip-chip interconnenctions," *Proceedings of the COMSOL Conference 2009 Milan* (2009).